Available online at www.sciencedirect.com
ScienceDirect
C. R. Mecanique 334 (2006) 483–492
COMPTES RENDUS MECANIQUE
http://france.elsevier.com/direct/CRAS2B/

Observation, analysis and modelling in complex fluid media

Iso-scalar surfaces, mixing and reaction in turbulent flows

César Dopazo [a,*], Jesús Martín [a], Juan Hierro [a,b]

[a] *Centro Politécnico Superior, Área de Mecánica de Fluidos, Universidad de Zaragoza, Maria de Luna, 3, 50018 Zaragoza, Spain*
[b] *Mechanical Engineering Department, The Johns Hopkins University, 3400 North Charles St. Baltimore, MD 21218, USA*

Available online 1 September 2006

Abstract

Turbulent scalar mixing with chemical reaction is investigated in terms of the local geometrical features of the iso-scalar surfaces—'scalar field topologies'—, using Direct Numerical Simulation data. Two scalars with identical initial distribution, one inert and the other obeying a prescribed Arrhenius-like chemical reaction, evolve in homogeneous isotropic turbulence with a mesh size 256^3. The two local principal curvatures, k_1 and k_2, of the iso-scalar surface at each point are straightforwardly obtained from the curvature tensor, $n_{i,j}$, whose elements are the spatial derivatives of the unit vector normal to the iso-surface. The scalar diffusive flux is decomposed into a 'flat-front' contribution plus a curvature induced molecular transport. Expressions for the normal propagating velocity relative to the fluid of iso-surfaces, of both the inert and the reactive scalar fields, are provided making use of the previous decomposition. The 'flat-front' and the curvature induced contributions to the diffusive fluxes, beside to the chemical reaction rate, are correlated with the principal curvatures. Results, including the joint statistics of the principal curvatures and their correlations with the scalar dissipation, are also presented. ***To cite this article: C. Dopazo et al., C. R. Mecanique 334 (2006).***

Résumé

Surfaces iso-scalaires, mélange, et réaction dans des écoulements. Le mélange turbulent de scalaires en présence de réaction chimique est considéré en termes de caractéristiques géométriques locales de surfaces iso-scalaires—« topologies de champs scalaires »—, à partir de données de simulations numériques directes. Deux scalaires de distributions initiales identiques, un inerte et l'autre obeissant à une réaction chimique prescrite du type Arrhenius, évoluent dans une turbulence homogène et isotrope sur une grille 256^3. Les deux courbures principales, k_1 et k_2, des surfaces iso-scalaires en chaque point sont obtenus directement à partir du tenseur de courbure, $n_{i,j}$, dont les éléments sont les dérivées spatiales du vecteur unitaire normal à l'iso-surface. Le flux diffusif du scalaire est décomposé en une contribution 'front-plat' et un transport moléculaire induit par la courbure. Les expressions pour la vitesse de propagation normale par rapport au fluide des iso-surfaces, des champs scalaires réactif et inerte, sont données en utilisant la décomposition précédente. Le 'front-plat' et les contributions induites par effet de courbure aux flux diffusifs, à côté du taux de réaction chimique, sont corrélés aux courbures principales. Des résulats incluant les statistiques conjointes des courbures principales et leurs corrélations avec la dissipation scalaire sont aussi présentées. ***Pour citer cet article : C. Dopazo et al., C. R. Mecanique 334 (2006).***

Keywords: Turbulence; Turbulent reacting flows; Scalar mixing; Direct Numerical Simulation; Curvature

Mots-clés : Turbulence ; Écoulements turbulents réactifs ; Mélange d'un scalaire ; Simulations Numériques Directes ; Courbure

* Corresponding author.
E-mail address: dopazo@unizar.es (C. Dopazo).

1631-0721/$ – see front matter
doi:10.1016/j.crme.2006.07.004

1. Introduction

The turbulent mixing of scalar fields (for example, temperature or inert/reactive species mass fractions) is a commonplace in energy systems and chemical processes. Strong fluctuations in space and time of the thermochemical variables complicate their mathematical description. Scalar heterogeneities are caused by the initial and boundary conditions, as well as induced by the chaotic velocity field.

Fully premixed systems can be characterised by a single reaction progress scalar variable and iso-surfaces can be identified within the reaction zone. Initially flat iso-scalar surfaces, such as those within premixed flames, can develop curvature through front instabilities (Pelcé et al. [1] and references therein) or significantly deform due to turbulent strain and rotation [2].

The time evolution of an non-material infinitesimal element of area, δA, can be expressed as

$$\frac{1}{\delta A}\frac{\mathrm{d}(\delta A)}{\mathrm{d}t} = (\delta_{ij} - n_i n_j)S_{ij} + V\nabla\cdot\mathbf{n} \tag{1}$$

where δ_{ij} is the Kronecker unit tensor, $\mathbf{n}$ is the unit vector normal to δA, S_{ij} is the strain rate tensor, and V is the velocity of displacement or propagation of δA relative to the fluid. The first term on the right side is the, so-called, area stretch and the second is the variation of δA by the combined action of the displacement speed and the curvature [3]. δA can be, for example, an element of an iso-scalar surface. The mean curvature, H, of δA is related to $\nabla\cdot\mathbf{n}$ by

$$\nabla\cdot\mathbf{n} = 2H = (k_1 + k_2) = \left(\frac{1}{R_1} + \frac{1}{R_2}\right) \tag{2}$$

where k_1 and k_2 are the principal curvatures and R_1 and R_2 the principal radius of curvature. k_1 and R_1 (and, similarly, k_2 and R_2) are positive for a convex surfaces towards $\mathbf{n}$.

The investigation of the mixing and reaction features under the action of a turbulent flow, in terms of iso-surface curvatures, k_1 and k_2, is an attempt at relating these phenomena to the small-scale topology of the scalar field. Using k_1 and k_2 instead of H tries to unveil the three-dimensional structures which are hidden by the essentially two-dimensional diagnostic techniques. Moreover, when $H = 0$ there exists an ambiguity as this might imply either a flat iso-surface or a saddle point with $k_1 = -k_2$.

DNS have been used by several authors [4–9] in order to investigate the stretching, rotation and folding of inert and reactive scalar iso-surfaces. Chen and Im [5] have used a 2-D DNS with detailed chemical kinetics for unsteady premixed hydrogen/air flames in order to investigate the dependence of the burning velocity with tangential strain, curvature and stretch. Haworth and Poinsot [6] unveiled through DNS the significant influence of the Lewis number upon premixed flame characteristics. Pope et al. [7] obtained via DNS the curvature of material surfaces in isotropic turbulence, finding that the most probable structures with large curvatures are cylinders. Echekki and Chen [9] numerically simulated turbulent premixed stoichiometric methane/air flames, evaluating, among other things, the effects of strain rate and mean curvature upon radicals concentration and heat release. Chakraborty and Cant [8] have used DNS to investigate the influence of unsteady tangential strain rates and mean curvatures on premixed flame propagation.

Iso-surface curvature can also appear explicitly in the molecular diffusion term in the scalar conservation equation [10–12]. It is relevant to scrutinize the importance of that curvature upon scalar molecular diffusion, as modelling the latter gives rise to a difficult closure problem in turbulent mixing [12,13]. None of the existing molecular mixing models [12] incorporate the influence of curvature explicitly. This article is, also, aimed at quantifying those effects upon mixing.

Section 2 introduces the mathematical description of the turbulent mixing problem for both inert and chemically reactive scalars; the propagation velocity of non-material iso-surfaces is expressed in terms of normal and curvature-induced molecular diffusion and of chemical contributions; the curvature tensor, whose non-zero eigenvalues are the principal curvatures, is introduced. The DNS methodology is briefly presented in Section 3. Section 4 analyses the DNS results, emphasizing the influence of curvature upon relevant statistical variables. Some preliminary conclusions and recommendations for future work are contained in Section 5.

2. Mathematical formulation

The scalar field evolution obeys the equation

$$\frac{\partial Y}{\partial t} + u_j\frac{\partial Y}{\partial x_j} = \frac{1}{\rho}\nabla\cdot(\rho D\nabla Y) + W(Y) \tag{3}$$

where Y is the mass fraction of reactants, varying from 1 in the pure reactive mixture to 0 in the fully reacted products. ρ is the fluid density, assumed constant, and D denotes the Fickian molecular diffusion coefficient. $W(Y)$ stands for the chemical conversion term; it is taken as 0 for an inert scalar or approximated as $W(Y) = -14Y(1-Y)^5$ for a reactive field. The latter has been used by Borghi and co-workers [14] in order to numerically mimic the chemical term for a premixed system. The numerical coefficient 14 has been chosen as to have Damköhler numbers of order unity. u_j is the jth component of a statistically homogeneous turbulent velocity vector field with zero mean, governed by the equations

$$\frac{\partial u_i}{\partial x_i} = 0 \tag{4}$$

$$\frac{\partial u_i}{\partial t} + u_j \frac{\partial u_i}{\partial x_j} = -\frac{1}{\rho}\frac{\partial p}{\partial x_i} + \nu \frac{\partial^2 u_i}{\partial x_j \partial x_j} + f_i \tag{5}$$

where p is the pressure, ν is the kinematic viscosity and f_i is the random forcing required to maintain the statistical stationarity of $\mathbf{u}$.

An iso-scalar surface, $Y(x,t) = const$, evolves according to the equation

$$\frac{\partial Y}{\partial t} + u_j \frac{\partial Y}{\partial x_j} = -V|\nabla Y| \tag{6}$$

where V is the iso-surface displacement or propagation velocity relative to the fluid, namely,

$$\mathbf{u}^y - \mathbf{u} = V\mathbf{n} \tag{7}$$

$\mathbf{u}^y$ is the absolute velocity of the iso-surface and $\mathbf{n}$ is the unit vector normal to $Y(x,t) = const$, defined by

$$\mathbf{n} = \frac{\nabla Y}{|\nabla Y|} \tag{8}$$

$\mathbf{n}$, thus, points towards the reactants side.

Equating the right sides of (3) and (6), deriving the first term of the right side of (3) as a product of ρD times ∇Y and using definition (8), one can easily obtain

$$V = -\frac{1}{\rho}\mathbf{n}\cdot\nabla(\rho D) - \frac{1}{|\nabla Y|} D\mathbf{n}\cdot\nabla|\nabla Y| - D(\nabla\cdot\mathbf{n}) - \frac{1}{|\nabla Y|}W(Y) \tag{9}$$

As $\mathbf{n}\cdot\nabla = \frac{\partial}{\partial x_n}$, x_n being the coordinate in the normal direction to the iso-surface, an equivalent expression for Eq. (9) is

$$V = -\frac{1}{\rho}\frac{\partial \rho D}{\partial x_n} - \frac{1}{\partial Y/\partial x_n} D\frac{\partial^2 Y}{\partial x_n^2} - D(\nabla\cdot\mathbf{n}) - \frac{1}{\partial Y/\partial x_n}W(Y) \tag{10}$$

The first term of (9) or (10) is the contribution to the propagation velocity of the variation of ρD normal to the iso-surface. In a premixed flame, ρ decreases when moving from the reactants to the products, while D increases. For the present case, ρ and D are taken as constants and this term vanishes. Eq. (10) has also been derived by Echekki and Chen [15].

The second term of (10) is the contribution to V of the normal molecular diffusion, denoted by V_n. $\partial Y/\partial x_n$ is positive, as x_n increases in moving from the products to the reactant sides. The sign of this contribution, therefore, depends on that of $\partial^2 Y/\partial x_n^2$, that is, on the curvature of the local profile, $Y(x_n)$, the scalar variation normal to the iso-surface. If there is an inflection point of $Y(x_n)$ at x_n^*, where $\partial^2 Y/\partial x_n^2 = 0$, this occurs for a particular iso-surface, $Y(x,t) = Y(x_n^*, t)$. For monotonically varying $Y(x_n)$, $\partial^2 Y/\partial x_n^2 > 0$ for $0 < Y(x_n) < Y(x_n^*)$, and V_n will be negative; for $Y(x_n^*) < Y(x_n) < 1$, $\partial^2 Y/\partial x_n^2 < 0$ and V_n will be positive. At x_n^*, $V_n = 0$. There might exist points at which $\partial Y/\partial x_n = 0$, and there V tends to infinity. It might be tempting to define a normal characteristic length scale, l_n, as $l_n = (\partial Y/\partial x_n)/(\partial^2 Y/\partial x_n^2)$; however, this is an ill-defined variable as it might take values in the range $(-\infty, +\infty)$.

The third term of (10) is the contribution to the propagation speed due to the spatial curvature of the iso-scalar surfaces, denoted by V_c. For iso-surfaces convex towards the reactants, $\nabla\cdot\mathbf{n} > 0$ and V_c is negative; if $Y(x,t) = const$ is concave towards the reactants side, $\nabla\cdot\mathbf{n} < 0$ and V_c is positive. Note that the values of the principal curvatures, k_1 and k_2, do not explicitly enter the definition of V_c.

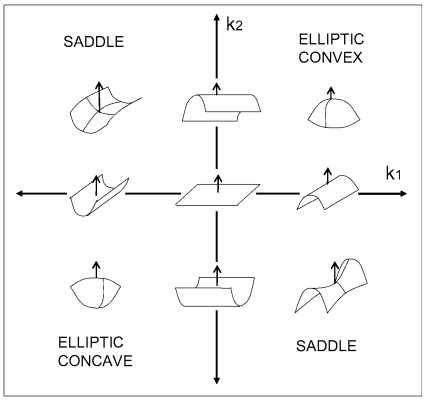

Fig. 1. Geometrical features associated to the principal curvatures, (k_1, k_2).

Fig. 1. Caractéristiques géométriques associées aux courbures principales, (k_1, k_2).

For Borghi's reaction rate, the last term in (10), the chemical contribution to V, named as V_{ch}, is always positive.

The principal curvatures, k_1 and k_2, are the two eigenvalues, different from zero, of the curvature tensor, $n_{i,j}$. From definition (8), one can readily obtain

$$n_{i,j} = \frac{1}{\partial Y/\partial x_n}(\delta_{ik} - n_i n_k)\frac{\partial^2 Y}{\partial x_j \partial x_k} \tag{11}$$

k_1 and k_2 can, then, be easily calculated. Fig. 1 depicts the geometry of the local small-scale scalar field structures in the principal curvature plane, (k_1, k_2). It is worth pointing out that a complete description of the local scalar field must also include its variation, $Y(x_n)$, in a direction normal to the iso-surface.

3. Numerical simulation

The velocity field, for a constant density fluid, is statistically homogeneous and isotropic and undergoes a random forcing producing a statistically stationary flow. Two different scalar fields evolve without forcing from an almost completely unmixed initial condition, with mean 0.5 and variance 0.17; the first scalar is inert, while the second is reactive with the chemical conversion rate specified after Eq. (3). The chemistry is, thus, modelled by a one step reaction transforming the premixed fuel into products; this expression closely resembles an Arrhenius-like reaction rate and is much faster to compute. The aim is to compare the effect of diffusion with that of diffusion and chemistry.

Direct Numerical Simulation (DNS) of the previous systems are performed in a cubic, 256^3, grid with periodic boundary conditions. The length of each edge of this cube is 2π. A second-order Runge–Kutta numerical scheme is used to advance the Navier–Stokes equations in time, whereas a pseudospectral code is used in the spatial domain.

The forcing scheme is that of Eswaran and Pope [16] with a zero correlation time of the forcing. To be more specific, all the wave numbers with a modulus less than $2\sqrt{2}$, except the zero node which has no contribution, receive each time step a random, white noise forcing contribution, whose phase is adjusted to enforce incompressibility and its intensity is such that the Reynolds number (based on the Taylor microscale) is close to 55.

The Damköhler number was chosen approximately equal to one, so that characteristic time and spatial scales due to chemistry are of the same order than those due to turbulent mixing. This saves the numerical complexity of solving a stiff problem with widely different characteristic scales. The Schmidt number was set equal to 0.7, less than unity, causing the scalar fields to develop slightly smaller characteristic scales than the velocity field.

The time step is chosen as the smallest value between 0.001, value selected in order to yield a well resolved chemical term, and the one which guarantees a Courant number, $C_0 = \mathrm{d}t/[\mathrm{d}x/\max\{|u_1|, |u_2|, |u_3|\}]$, equal to 0.8.

The initial velocity field evolves for ten eddy turn-over times to guarantee that it had reached a stationary state where the spectrum presents small fluctuations. Then, an initial scalar field, as close as possible to a homogeneously random distribution of values 0 and 1, is selected. The initial mean is close to 0.5 and the scalar is smoothed about 0 and 1 to avoid strong numerical dispersion during the initial time steps. The inert and the reactive scalar fields are

initially identical, then it is assumed an instant ignition in the reactive case. This is an idealization, as the focus of this paper lies on the interaction of chemistry with homogeneous turbulence.

4. Results

The full characterisation of the velocity field at any time is provided by the following quantities: Taylor Reynolds number, $Re_\lambda = 47.6$, integral length scale, $l_{\text{int}} = 0.89$, viscosity value, $\nu = 0.012$, Taylor microscale, $\lambda = 0.44$, Kolmogorov microscale, $\eta = 0.033$, kinetic energy dissipation rate, $\varepsilon = 1.52$, root mean square velocity, $\langle k \rangle = 1.29$ and the maximum wave number times the Kolmogorov microscale, $k_{\max}\eta = 3.98$.

Analogously, to characterize the scalar fields, the following variables are used: diffusivity coefficient, $D = 0.017143$, for the two scalar fields. The data presented here are taken at a time when the means of the inert and reactive scalars, $\langle Y \rangle$ are close to 0.5 and 0.25, respectively, with variances, $\langle Y'^2 \rangle$, 0.055 and 0.089. The time was chosen so that the memory from the initial condition was already lost, although strong fluctuations in the scalar field remained.

The probability density function (pdf) of both the inert and the reactive scalars are presented in Fig. 2. While the inert field approximately maintains its symmetry with respect to the constant mean, $\langle Y \rangle = 0.5$, the reactive scalar values, with $\langle Y \rangle = 0.25$, move towards zero, due to its depletion by the chemical consumption.

The balance of the different terms in Eq. (3) conditioned to the value Y at particular iso-surfaces appears in Fig. 3 for both inert (Fig. 3(a)) and reactive (Fig. 3(b)) fields. The curvature induced diffusion is smaller than the normal diffusion, although non negligible, for both the inert and the reactive cases; the curvature diffuses anti-symmetrically about the mean scalar value for inert species; on the other hand, for reactive fields the curvature diffusion seems to act predominantly for $Y > 0.16$, being more intense for scalar values where the chemical conversion is relatively small. The chemistry is likely to cause strong normal variations of the scalar, producing large values of $\partial^2 Y/\partial x_n^2$. In Fig. 3(c) the sum of the 'flat front' and the chemical term conditional upon Y is plotted. This quantity is of interest since it is the only one present in a flat laminar flame [17] and could be used to model flames as flamelets with curvature induced perturbations.

Fig. 4 displays the propagation velocity, V, as well as the normal contribution, V_n , the curvature induced speed, V_c, and the chemical displacement velocity, V_{ch}. For the inert case Fig. 3(a), negative and positive velocities, V, V_n and V_c, occur for scalar values below and above the mean, respectively. The curvatures of the iso-surfaces, $\nabla \cdot \mathbf{n}$, and the normal scalar profile, $Y(x_n)$, are both negative for $Y > 0.5$ and positive for $Y < 0.5$. Therefore, iso-surfaces with concavity towards the reactant side are associated to the negative curvature zone of $Y(x_n)$, resulting in positive propagation velocities. On the other hand, an iso-surface convex towards the reactants propagates with a negative speed and usually occur in regions of positive curvature of $Y(x_n)$. Chemistry significantly modifies the previous picture; the propagation velocity induced by the chemical conversion is always positive, as already discussed, and larger for scalar values with strong chemical activity, monotonically decreasing as Y increases towards unity. V_n losses

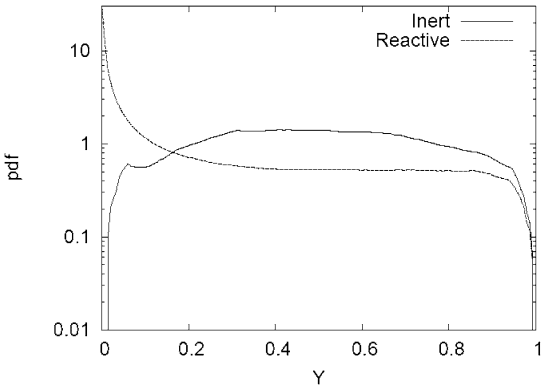

Fig. 2. Scalar probability density function at the selected time.

Fig. 2. Fonction densité de probabilité des scalaires au temps sélectionné.

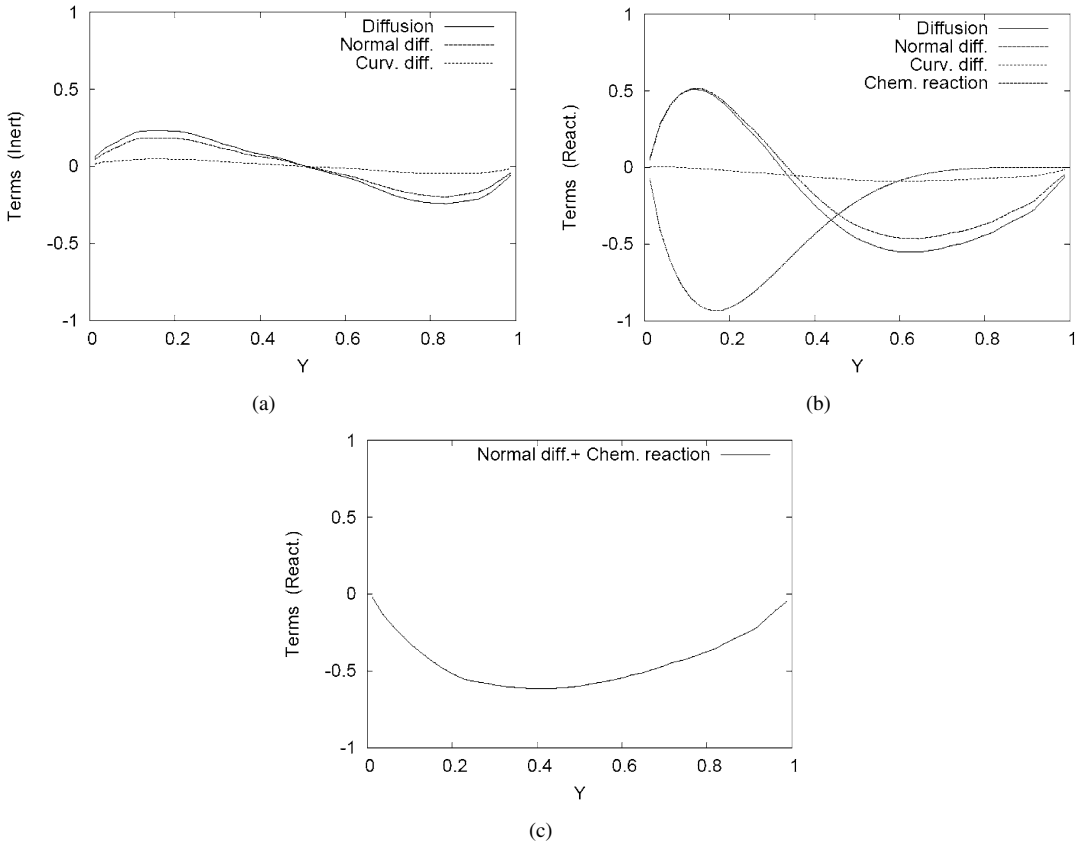

Fig. 3. The diffusion term, its normal and curvature parts, and the chemical reaction as a function of the scalar mass fraction: (a) inert; (b) reactive; (c) summation of the normal diffusion and the chemical reaction terms for the reactive scalar.

Fig. 3. Terme de diffusion, ses parties courbe et normale, et la réaction chimique en fonction de la fraction massique scalaire : (a) inerte ; (b) réactif ; (c) sommation de la diffusion normale et des termes de réaction chimique pour le scalaire réactif.

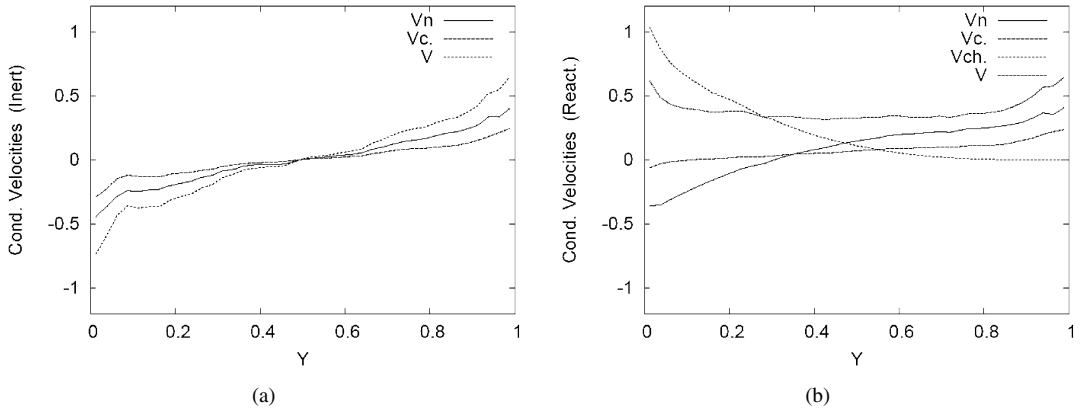

Fig. 4. Propagation velocities, V, V_n, V_c and V_{ch}, of all the iso-scalar surfaces as a function of the scalar mass fraction: (a) inert; (b) reactive.

Fig. 4. Vitesses de propagation, V, V_n, V_c et V_{ch}, de toutes les surfaces iso-scalaires en fonction de la fraction massique scalaire : (a) inerte ; (b) réactif.

its anti-symmetry with respect to $Y = 0.5$, being negative (positive curvature of $Y(x_n)$) for $Y < 0.35$, approximately, and positive for $Y > 0.35$. V_c is comparable to V_n; for $Y > 0.30$, it becomes positive with larger values in the slow chemistry region.

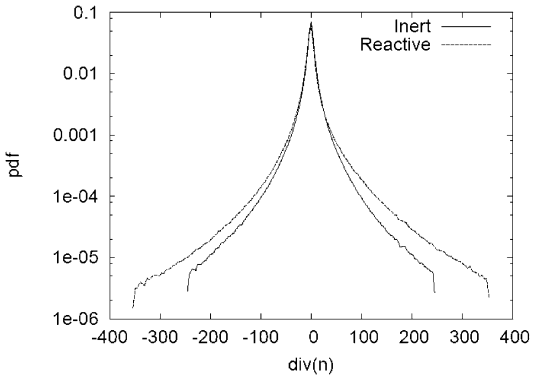

Fig. 5. Mean curvature probability density function, for all scalar iso-surfaces.

Fig. 5. Fonction densité de probabilité de la courbure moyenne, pour toutes les iso-surfaces scalaires.

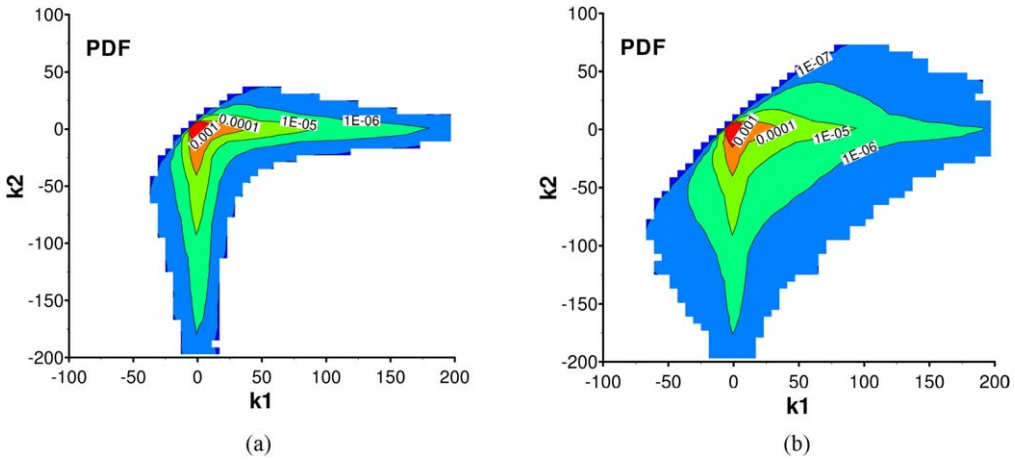

Fig. 6. Joint probability density function of the principal curvatures: (a) inert; (b) reactive, for all scalar iso-surfaces.

Fig. 6. Fonction densité de probabilité conjointe des courbures principales : (a) inerte ; (b) réactif, pour toutes les iso-surface scalaires.

The pdf of the mean curvature, $\nabla \cdot \mathbf{n}$, of all iso-surfaces (all values of Y) is plotted in Fig. 5, for both the inert and the reactive cases. While the inert scalar displays a symmetric pdf, that of the reactive field shows a moderate skewness to the right, indicating that iso-surfaces with convexity towards the reactants are slightly more probable.

Fig. 6 depicts the joint pdf of the principal curvatures, k_1 and k_2, of all iso-surfaces for inert Fig. 6(a) and reactive Fig. 6(b) scalars. The most probable values cluster around (0, 0), namely, flat iso-surface; the shape of the joint pdf tails indicate a tendency to observe elongated structures with curvature, either positive or negative, only in one direction. On the other hand, the chemistry induces curvatures in a much wider range than that for the inert case.

In Fig. 7, the scalar dissipation rate, ε_c, is represented in terms of k_1 and k_2. Comments similar to those for Fig. 6 can be made. Moreover, while the inert case presents a clear symmetry for convex and concave structures, the reactive scalar shows a slight preference for the dissipative concave iso-surfaces.

The terms on the right side of Eq. (3), conditioned upon the values of k_1 and k_2, are displayed in Fig. 8 for a reactive scalar. Molecular diffusion (Fig. 8(a)), as well as its normal (Fig. 8(b)) and curvature (Fig. 8(c)) contributions are presented. Molecular diffusion, as well as its normal and curvature contributions, display a preferential action over elongated structures, convex towards the reactants. The most intense reaction occurs for both convex and concave elongated iso-surface elements.

Fig. 9 is a plot of V, V_n, V_c and V_{ch} conditional upon k_1 and k_2 for all scalar iso-surfaces of the reactive scalar. As the mean curvature is the sum of k_1 and k_2, the conditional curvature diffusive contribution is constant in lines $k_1 + k_2 = const$. The normal contribution, surprisingly, presents also bands with similar trend. On the other hand,

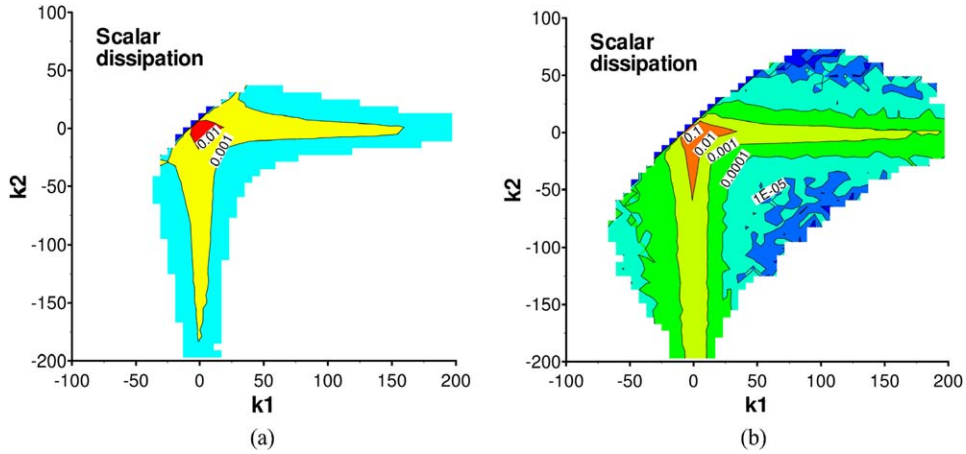

Fig. 7. Scalar dissipation rate conditioned upon the principal curvatures: (a) inert; (b) reactive, for all scalar iso-surfaces.

Fig. 7. Taux de dissipation scalaire conditionné par les courbures principales : (a) inerte ; (b) réactif, pour toutes les iso-surface scalaires.

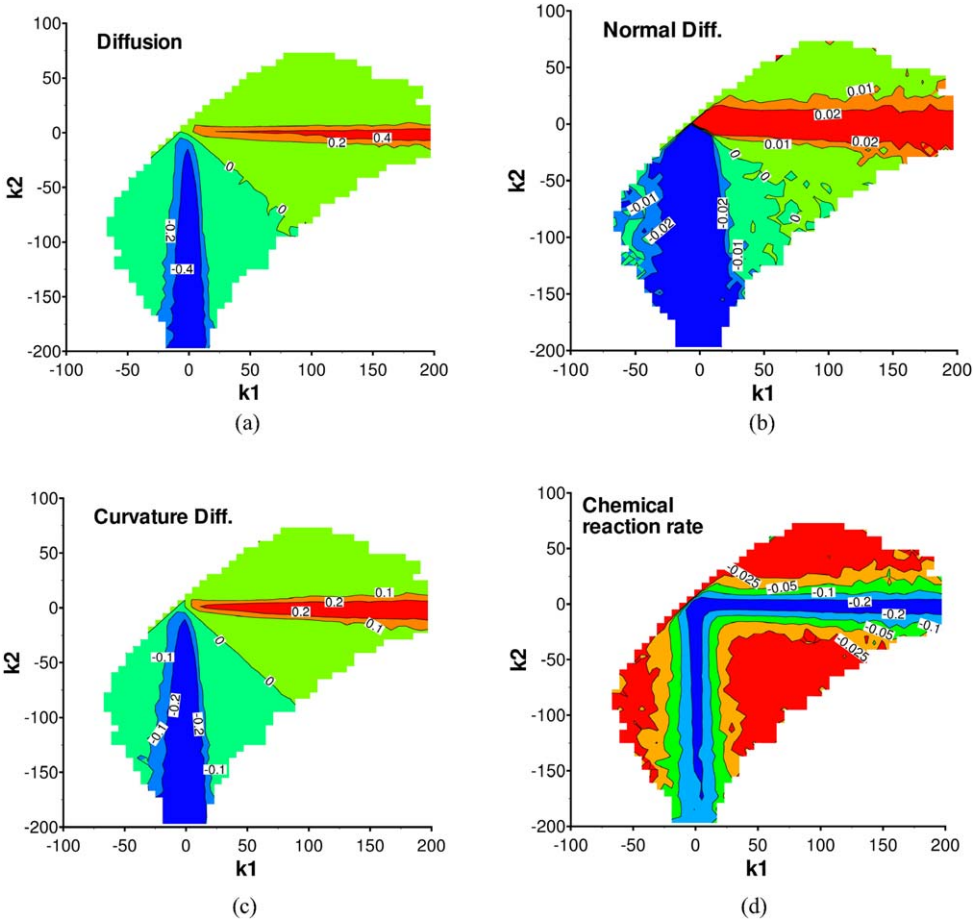

Fig. 8. (a) Reactive scalar molecular diffusion, (b) normal diffusion, (c) curvature-induced diffusion and (d) chemical reaction rate, conditioned upon the principal curvatures, for all scalar iso-surfaces.

Fig. 8. (a) Diffusion moléculaire du scalaire réactif, (b) diffusion normale, (c) diffusion induite par la courbure, et (d) taux de réaction chimique, conditionnée aux courbures principales, pour toutes les iso-surface scalaires.

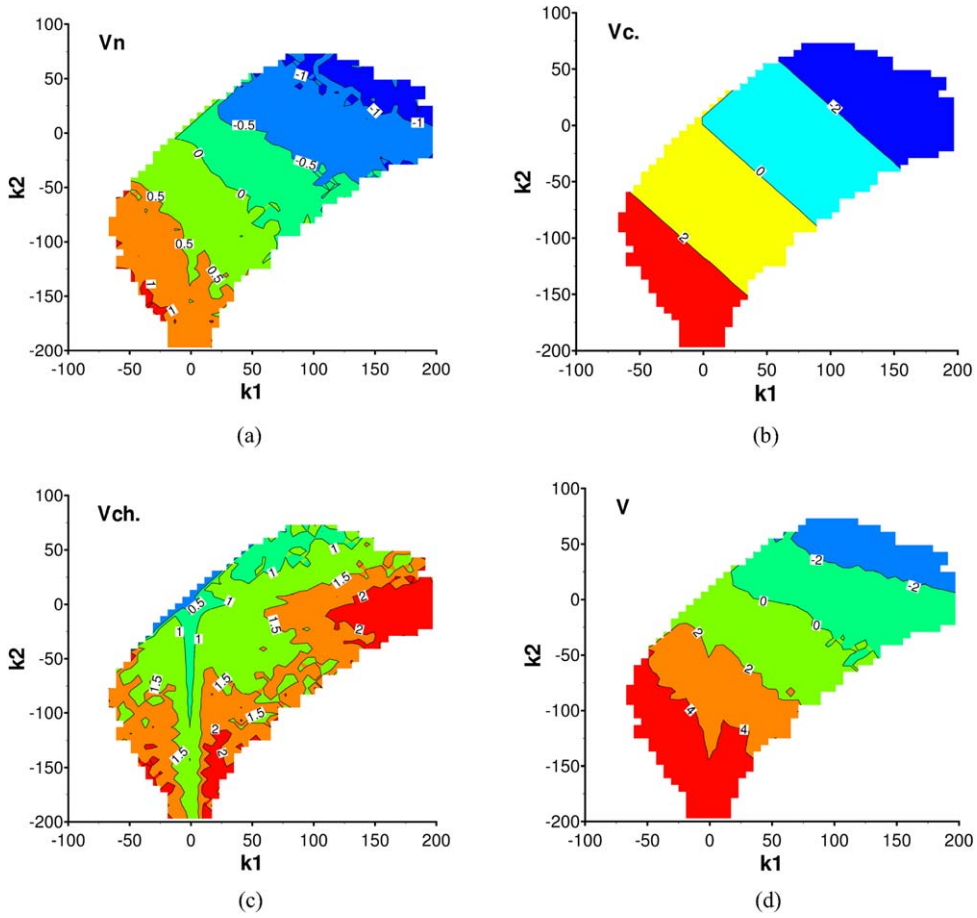

Fig. 9. Reactive scalar velocities of propagation: (a) V_n, (b) V_c, (c) V_{ch}, (d) V, for all scalar iso-surfaces.

Fig. 9. Vitesses de propagation du scalaire réactif : (a) V_n, (b) V_c, (c) V_{ch}, (d) V, pour toutes les iso-surface scalaires.

the chemical contribution displays a more complex structure, appearing its highest values correlated with iso-surface geometries having large values of one of the principal curvatures with simultaneous negligible values of the other one, that is: the highest values of V_{ch} appear near of the axes and far from the origin. This remarkable characteristic awaits further confirmation and interpretation.

5. Conclusions

The results of a 256^3 DNS for inert and reactive scalars in a constant density fluid set in motion by a statistically homogeneous field of turbulence have been used to describe mixing characteristics in terms of mean and principal curvatures. The preferred small-scale scalar geometric structures emerge from these preliminary studies. Flat and cylinder-like (one principal curvature near zero and the other one either positive or negative) fronts are apparently the most probable iso-surfaces.

Higher resolution DNS would be required in order to improve the statistics quality. Future work should definitely investigate variable density turbulence with either simple chemistry or moderately complicated kinetics. The curvature characterisations in the present work for all scalar values should be particularised to individual iso-surfaces. The snapshots presented in the present investigation should be extended to consider the scalar statistics time evolution and, therefore, the iso-surfaces geometry temporal variation. A possible and probable relationship between the small-scales of the turbulent flow and of the scalar field should be explored. Last, though not least, the effect of curvatures upon molecular mixing is a topic of interest, mainly to try to include it, if relevant, in new molecular mixing models.

References

[1] P. Pelcé (Ed.), Dynamics of Curved Fronts, Academic Press, Inc., 1988.
[2] W. Kollmann, J.H. Chen, Pocket formation and the flame surface density equation, in: 27th Symp. (Internat.) on Combust., The Combustion Institute, Pittsburgh, 1998, p. 927.
[3] S.M. Candel, T.J. Poinsot, Flame stretch and the balance equation for the flame area, Combust. Sci. Technol. 70 (1990) 1–15.
[4] G. Brethouwer, Mixing of passive and reactive scalars in turbulent flows. A numerical study, PhD Dissertation, Tech. Univ. Delft, Ponsen & Looijen, The Netherlands, 2000.
[5] J.H. Chen, H.G. Im, Stretch effects on the burning velocity of turbulent premixed hydrogen/air flames, in: 28th Symp. (Internat.) on Combust., The Combustion Institute, Pittsburgh, 2000, p. 211.
[6] D.C. Haworth, T.J. Poinsot, Numerical simulations of Lewis number effects in turbulent premixed flames, J. Fluid Mech. 244 (1992) 405–436.
[7] S.B. Pope, P.K. Yeung, S.S. Girimaji, The curvature of material surfaces in isotropic turbulence, Phys. Fluids A 1 (1989) 2010–2018.
[8] N. Chakraborty, S. Cant, Unsteady effects of strain rate and curvature on turbulent premixed flames in an inflow–outflow configuration, Combust. Flame 137 (2004) 129–147.
[9] T. Echekki, J.H. Chen, Unsteady strain rate and curvature effects in turbulent premixed methane/air flames, Combust. Flame 106 (1996) 184–202.
[10] C. Dopazo, Recent developments in PDF methods, in: P.A. Libby, F.A. Williams (Eds.), Turbulent Reacting Flows, Academic Press, London, 1994, pp. 375–474.
[11] C. Dopazo, J. Martin, J.P. Hierro, Turbulent mixing and combustion, in: 2nd Mediterranean Combust. Symp., Invited paper, Sharm-El-Sheik, January 6–11, 2002.
[12] C. Dopazo, J. Martin, J. Hierro, The influence of iso-scalar surface curvature on turbulent mixing and reaction, in: Simplicity, Rigor and Relevance in Fluid Mechanics. A Volume in Honor of Amable Liñán, CIMNE, Barcelona, 2004, pp. 187–214.
[13] L. Vervisch, E. Bidaux, K.N.C. Bray, W. Kollmann, Surface density function in premixed turbulent combustion modelling. Similarities between probability density function and flame surface approaches, Phys. Fluids 10 (7) (1995) 2496–2503.
[14] A. Picart, R. Borghi, J.P. Chollet, Numerical simulation of turbulent reacting flows, in: 10th Internat. Symp. on Turbulence, Univ. of Rolla, Missouri, 1986.
[15] T. Echekki, J.H. Chen, Analysis of the contribution of curvature to premixed flame propagation, Combust. Flame 118 (1999) 308–311.
[16] V. Eswaran, S.B. Pope, Direct numerical simulation of the turbulent mixing of a passive scalar, Phys. Fluids 31 (1988) 506–520.
[17] N. Peters, The turbulent burning velocity for large scale and small scale turbulence, J. Fluid Mech. 384 (1999) 107–132.